Research article Available online www.ijsrr.org ISSN: 2279–0543

International Journal of Scientific Research and Reviews

Calcination of red soil and black soil used for the degradation of aniline blue dye

P. Muhambihai[1*], V. Rama[2] and P. Subramaniam[3]

[1] Aditanar College of Arts & Science,Tiruchendur, [2]Sarah Tucker College (Autonomous),Tirunelveli[*]E-mail id: muhaselva@gmail.com
Affiliated to ManonmaniamSundaranar University, Abishekapatti, Tirunelveli-627012, Tamil Nadu, India

ABSTRACT

The Photocatalytic degradation of Aniline blue dye (AB) was studied using calcinated red soil (CRS) and black soil (CBS) under sun light. The materials were characterized with XRD, FT-IR, SEM and EDS. Catalyst dosage, initial concentration of dye, time, electron acceptor and pH of the reaction mixture were examined. Photocatalytic processes worked better in acidic medium with pH value 1. The effect of the initial aniline blue concentration on the percentage degradation was also studied, demonstrating that the degradation of aniline blue generally increased when decreasing its concentration. The dye removal efficiency of the CRS is greater than that of CBS.

KEYWORDS: Aniline Blue dye (AB); Photocatalytic Degradation, Calcinated Red Soil (CRS), Calcinated black soil (CBS)

***Corresponding author**

P. Muhambihai

Aditanar College of Arts & Science,

TiruchendurTirunelveli

E-mail id: muhaselva@gmail.com

INTRODUCTION

Textile industries have shown a significant increase in the use of synthetic complex organic dyes as coloringmaterials. Dyes after use by various industries, are discharged to the water bodies like river, ponds etc. Thus, they become potential pollutants and need effective treatment. It has long been known that the oxidation of metals such as iron, tin and zinc can bring about the reduction of halogenated organics. Different processes for colour removal typically include physical, chemical and biological schemes.Dyes are usually difficult to biodegrade. A large degree of aromaticity present in modern dye molecules increases stability, and conventionalbiological treatments are ineffective for decolorization and degradation. Furthermore, a large fraction of dyes is adsorbed on the sludge and is not degraded. Ozonation and chlorination are also used for the removal of certain dyes, but at slower rates. They often have high operating costs and limited effect on carbon content. Advanced oxidation processes (AOPs) are potential to overcome many of these limitations.Photocatalysis is a phenomenon that occurs when a reaction chain is taking place in the presence of light and solid catalyst in the solution[7].Photocatalyst is also called photochemical catalyst and the function is similar to the chlorophyll in the photosynthesis. In a photocatalytic system, photo-induced molecular transformation or reaction takes place at the surface of catalyst (**Fig.1**). Specifically, under the ultraviolet light or sunlight, photocatalytic reaction may produce negative electron (e−) in the conduction band and positive hole (h+) in the valance band of a semiconductor. e− and h+ are powerful reductive and oxidizing agents. Then oxidation-reduction reaction was induced by e− and h+ [8,9]. Holes oxidize H_2O on the surface of semiconductors and ·OH is photogenerated. O_2 on the surface of semiconductors traps electron and $O_2^{\cdot-}$ and O_2^{2-} are formed. These reactive oxygen species (ROS) (e.g. $O_2^{\cdot-}$, O_2^{2-} and ·OH) exhibit high oxidative activity for organic compounds. They can readily cleave C-C bond, lead to a partial or total decomposition, and mineralize into CO_2, H_2O and inorganic ion (e.g. Cl^-, NO_3^-, SO_4^{2-}) [10,11]. There are many catalysts reported in the literature for this exciting process. Among these metal oxides (TiO_2, ZnO, SnO_2 and CeO_2), which are abundant in nature, have also been extensively used as photocatalysts, particularly as heterogeneous photocatalyst since several decades . Heterogeneous photocatalysis employing metal oxides such as TiO_2, ZnO, SnO_2 and CeO_2 has proved its efficiency in degrading a wide range of distinct pollutants into biodegradable compounds and eventually mineralizing them to harmless carbon dioxide and water[13, 14]. In this paper, iron oxide rich Calcinated red and black soils were used as the photocatalyst for the degradation of aniline blue dye. Therefore, in order to minimize the high cost and the difficulty of regeneration, a search for cheap, effective catalyst such as sand derivatives is desirable.

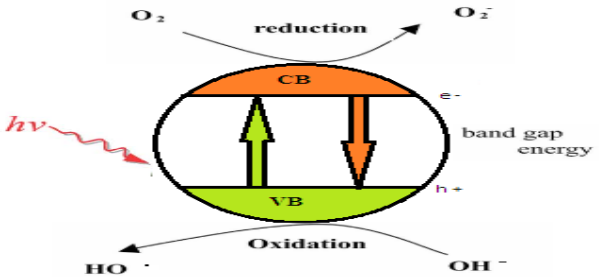

Fig.1. Schematic representation of Photo induced Molecular Transformation

EXPERIMENTAL

Calcinations of Red soil (CRS) and Black soil (CBS)

Red and Black soils were collected from Kayamozhi and Ottapidaram,Tuticorin District, Tamil nadu, India and their physical and chemical parameters are determined. pH, density and particle size distribution of the soil were determined and listed in table **1**. The collected raw soils were washed with deionized water for several times. If not washing like that it could not remove the soil dust as well as other undesired particles. It was dried at 100 ^{0}C for 2 hr and then crushed and sieved to obtain powder soil with a particle size less than 75 µm. These powder soils were calcinated at 300 ^{0}C for 2 hrs.

Table 1: Characteristics of CRS and CBS

Sl. No	Characteristics	Red Soil	Black Soil	Unit
1	Moisture content	5.25	7.39	%
2	BET Surface area	72.00	60.78	m^2/gm
5	pH	7.5	7.5	-
6	Specific gravity	2.92	2.25	gm/m3
7	Bulk density	1.75	1.538	gm/cm3
8	Porosity	0.7	0.5	-

Measurement of optical density

Elico model SL-164 UV- Vis spectrophotometer was used with quartz cell of 1cm path length for measuring the maximum wavelength for dyes.The Aniline blue (AB) was scanned from 250-800 nm wavelength range. The UV-Vis spectrum of Aniline blue is givenin **Fig.2**. The λ_{max} for Aniline Blue is 603 nm.

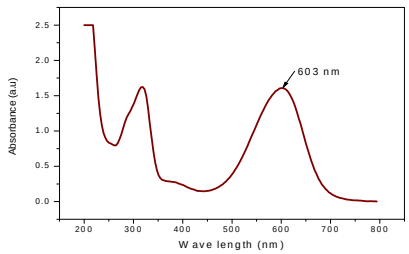

Fig.2.UV-Visible spectrum of Aniline Blue

DISCUSSION

Characterization of CRS and CBS

UV-Visible spectral study

UV-Vis absorption spectra and the Tauc plot of the prepared nanomaterials are shown in **Fig. 3**.Optical properties of the samples were studied by UV-Vis absorption spectroscopy. The absorption spectra of samples were recorded in the range 200 nm to 1200 nm by a UV-2600 spectrometer. The UV spectra for Calcinated Red soil in aqueous media displayed broad absorption peak at 408 nm which implies the lower particle size of Calcinated Red soil. In the UV Vis spectrum for Calcinated black soil, it should be noted that the absorption edge values for CBS samples lie in the wavelength range of 435 nm. The band gap energy (Eg) of the prepared materials can be evaluated from the UV-Vis spectra by Tauc plot of $(\alpha h\upsilon)^2$ versus $(h\upsilon)$ and extrapolation of the linear portions of the curves to the energy axis according to [15]:

$$\alpha h\upsilon = B(h\upsilon - E_g)^{1/2}$$

where α is the absorption coefficient, hv is the photon energy, E_g is the direct band gap energy, and B is a constant. The absorption coefficient (α) was determined from the relation $A = I/I_0 = e^{(-\alpha d)}$, or it can be calculated using the well-known relation deduced from Beer–Lambert's relation, α = 2.303A/d, where d is the path length of the quartz cuvette and A is the absorbance determined from the UV–visible spectrum. The estimated optical band gaps of CRS are about 3.0 eV and CBS are about 2.8 eV

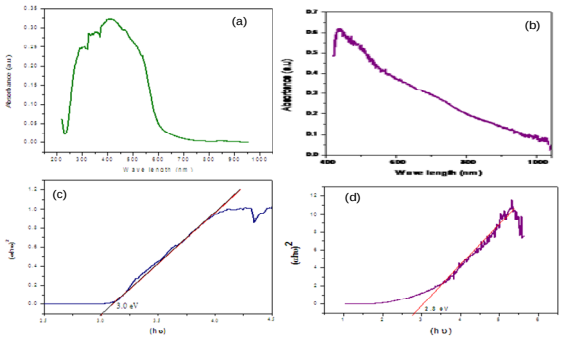

Fig.3. UV–Vis absorption spectra and Tauc plot of (a & c) CRS and (b & d) CBS

FT-IR spectral study

The FT-IR spectra for CRS and CBS are shown in **Fig.4.** In the FT-IR spectrum of Calcinated Red soil, the absorption peaks at 3406.28cm^{-1} and 2949.15 cm^{-1} are described to stretching vibrations of –OH groups. Peaks around 1200 cm-1 to 1500 cm^{-1} concluded the presence of C-H vibration of stretching band. The region 1315.45cm^{-1} represents C-O stretching. The smaller peaks in 1028.06cm^{-1} represent Si-O-Si [16] stretching frequency. The smaller peaks in

466.77cm^{-1}represent Fe-O[17]stretching frequency. The peaks at 877.61 cm^{-1} and 692.44 cm^{-1} were attributed to different Mg-O- Mg vibration modes of MgO[18]. The absorption band at wave number 516.92 cm^{-1} represents the Al-O[19] stretching mode. The wide and strong band at around 466.77 cm^{-1} corresponds to the Ca-O[20] bonds. This indicates the presence of Si, Al, Fe, Mg and Ca oxides are present in the Calcinated Red soil. In the FT-IR spectrum of Calcinated Black soil, the absorption peaks at 3406.28cm^{-1} and 2949.15 cm^{-1} are described to stretching vibrations of –OH groups. Peaks around 1200 cm-1 to 1500 cm^{-1} concluded the presence of C-H vibration of stretching band. The region 1315.45cm^{-1} represents C-O stretching. The smaller peaks in 1028.06cm^{-1} represent Si-O-Si stretching frequency. The smaller peaks in 466.77cm^{-1} represent Fe-O stretching frequency. The peaks at 877.61 cm^{-1} and 692.44 cm^{-1} were attributed to different Mg-O- Mg vibration modes of MgO. The absorption band at wave number 516.92 cm^{-1} represents the Al-O stretching mode. The wide and strong band at around 466.77 cm^{-1} corresponds to the Ca-O bonds. This indicates the presence of Si, Al, Fe, Mg and Ca oxides are present in the Calcinated Black soil.

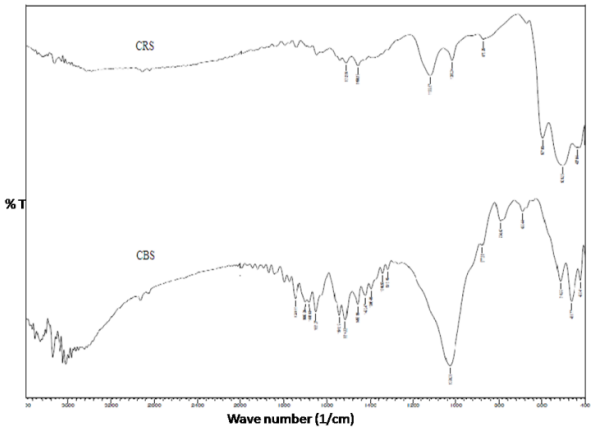

Fig.4. FT-IR spectrum of CRS and CBS

X-ray diffraction study

The X-ray diffraction of CRS and CBS are given in **Fig .5.** The phase and crystallinity of the prepared sample were investigated by x-ray diffraction patterns. X-Ray Diffraction (XRD) patterns obtained from X-Ray Diffractometer using 1.5406Å wavelength radiation were used to identify the composition and the same is used to calculate particle size using Debye– Scherrer equation.

$$D = 0.9\ \lambda/\beta\ \cos\theta$$

Where, 'D' is average particle size, 'λ' is wave length of X-Ray (0.1541 nm), 'β' is FWHM (full width at half maximum), 'θ' is the diffraction angle. The most intense peak of CRS at 2θ = 26.40˚ (2 1 1), 20.53˚ (1 0 0) and 67.50˚ (4 3 2) were obtained. The size of the CRS nanoparticles found to be 35 nm ranges. The sharpness, strong intensity and narrow width of CRS diffraction peaks in the XRD pattern indicate that the prepared CRS sample is well crystallized. The most intense peak

of CBS at 2θ = 26.69˚ (1 0 1), 68.04˚ (0 2 3) and 29.51˚ (2 2 0) were obtained which corresponds to SiO_2 and hematite phase of CRS and CBS. The size of the CBS nanoparticles found to be 37 nm ranges.

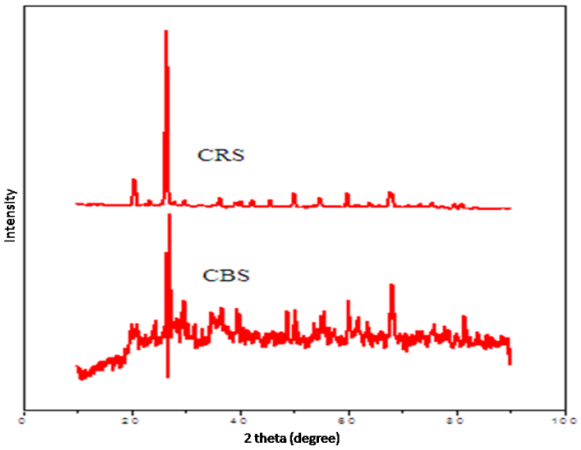

Fig.5. XRD pattern of CRS and CBS

SEM and EDS study

The SEM image of CRS and CBS are shown in **Fig.6**. The SEM image of CRS exhibits the particles were smoothly sphere shaped in appearance. This may be due to the presence of iron oxides, which might have added the flocculent nature to the calcinated Red soil and the size of the particles was measured by SEM using imagej. The average particle size of CRS was found to be 35.69 nm. The EDS analysis indicated that the Calcinated Red soil sample is mainly composed by Si, Al, O, Fe, Ca, Mg and Na. In the SEM image of CBS, it can be seen clearly that the particles are uniformly aggregated, spherical shaped and the size of the particles was measured by SEM using imagej. The average particle size of CBS was found to be 37.19 nm. The EDS analysis indicated that the Calcinated Black soil sample is mainly composed by Si, Al, O, Fe, Ca, Mg and Na.

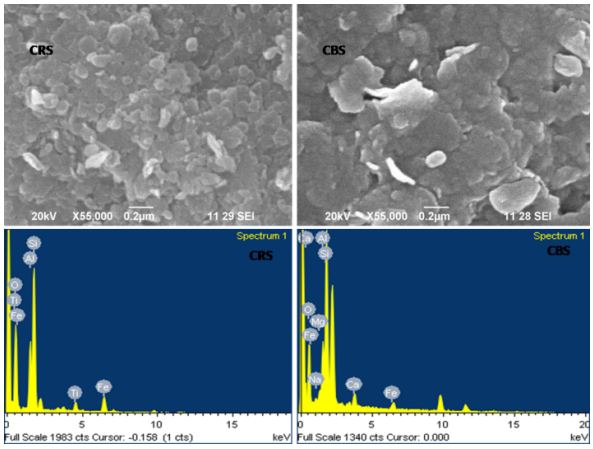

Fig.6. SEM and EDS pattern of CRS and CBS

TEM and SAED study

Figure 7a shows the TEM image and corresponding selected-area electron diffraction (SAED) pattern of the CRS. TEM image confirms the formation of CRS as nanoparticles and it has an average size of about 34.56 nm. The h k l indices measured using Selected Area Electron Diffraction (SAED) obtained from an polycrystalline of the CRS particles (Fig. 7b) correspond to the hematite and SiO_2phase in CRS (h k l) : (2 1 1), (3 1 1),(0 0 4), (4 3 0), (4 3 2) and (4 4 4). The TEM morphology of the CBS is shown in Fig. 7c: it is represented by agglomerate particles with a size of 37.2 nm; the orientation of crystallites is reflected in the circular SAED pattern (Fig. 7d). The measured h k l indices were (h k l) : (2 0 0), (0 1 4), (1 1 2) and (2 2 6) which corresponds to SiO_2 and hematite phase of CBS.

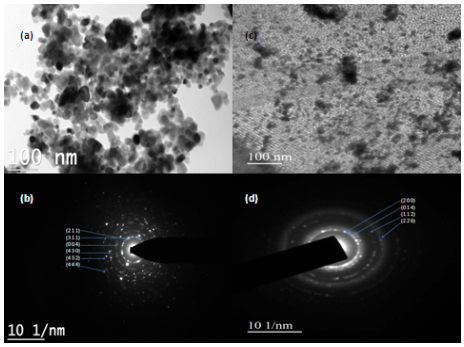

Fig.7. TEM and SAED pattern of (a & b) CRS and (c & d) CBS

Photocatalytic degradation of dyes by sunlight method

Effect of initial dye concentration on the photodegradation of dye

The effect of initial concentration of dyes on the percentage degradation is studied by varying the initial concentrations from 10 to 60 ppm in the case of AB dyes with optimum catalyst loading. The degradation efficiency decreases by increasing the concentration of the dye molecules for sunlight method. Due to the fact that as the concentration of dye molecule increases, more molecules get adsorbed on the photocatalyst (CRS and CBS) surface, the substrate concentration can influence the extent of adsorption and rate of reaction at the surface of the photocatalyst. It will be an important remitter for optimization between high degradation rate and efficiency[21] found the optimum propoxur concentration. Above this concentration, the rate decrease due to insufficient quantity of $OH^{\bullet}$ radicals, as the formation of $^{\bullet}OH$ radicals is a constant for a given amount of the catalyst. The experimental data showed that the percentage removal capacity for CRS are maximum compared to CBS. This is due to the fact that particle size for CRS nanocomposites are low compared to CBS.

Effect of photocatalyst loading on dye degradation

The effect of photocatayst loading on the percentage degradation of dyes has been studied by varying its amount from 0.01g - 0.09 g /50 ml of dye solutions. From the data, the % of degradation efficiency increases by increasing the amount of catalyst for the removal of AB by sunlight method. It is well documented that the initial rates of reaction are directly proportional to the mass (m) of catalyst[22].The increase in the efficiency seems to be due to the increase in the total surface area (namely number of active sites) available for the photocatalytic reaction as the dosage of photocatalyst increased.

Effect of pH on the photocatalytic degradation dyes

The effect of pH on the photodegradtion of dyes was studied by varying the pH of the medium and keeping the other factors as constant. In reality, the interpretation of pH effects on the efficiency of molecules photodegradation process is a very difficult task because three possible reaction mechanisms can contribute to the degradation, namely, hydroxyl radical attack, direct oxidation by the positive hole and direct reduction by the electron in the conducting band. It appears that the effect of pH on the degradation of the pollutants is variable and controversial since the positive holes are considered as the major oxidation species at low pH whereas hydroxyl radicals are considered as the predominant species at neutral or high pH levels.The result shows that about maximum degradation efficiency using both CBRS and CBS for the removal of AB dye at pH 1 and minimum at pH 11. The zero point charge (zpc) for CRS is 7.5 and 7.6 for CBS, This is due to the fact that the photocatalyst surface becomes + ve charged at pH < 7.5 for CRS and < 7.6 for CBS and vice versa making the electrostatic interaction between the dye and the catalyst surface predominant adsorption process. Hence the AB, anionic dye removals aremaximum at acidic pH.

Effect of variation of contact time on the photocatalytic degradation of dyes

The effect of contact time on the adsorption process was studied by varying the contact time and keeping the other factors as constant. It is evident that the percentage removal of dye increases with increasing irradiation time. This is became more $OH^{\bullet}$ radical will be generated when the exposure time is longer. The generation of $OH^{\bullet}$radicals is crucial. In photodegradation, $OH^{\bullet}$radicals as it oxidized the organic pollutants to carbon dioxide, water and some simple mineral acids.The optimum conduct time required for maximum removal was found to be 60 minutes for solar radiation.

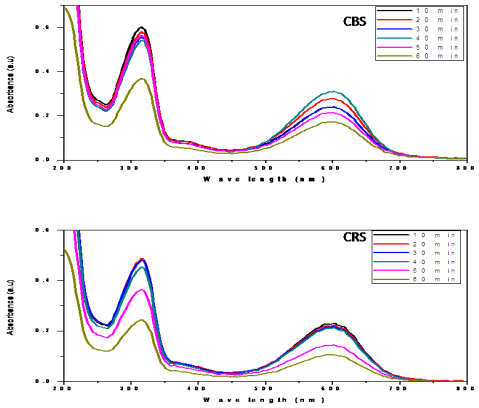

Fig.8. Photocatalytic degradation effect of CBS and CRS for AB dye removal under sunlight irradiation

Effect electron acceptors

(i) Effect of H_2O_2

The effect of H_2O_2 on the photodegradation of dyes was studied by addition of H_2O_2 and keeping the other factors as constant. In heterogeneous photocatalytic reaction, molecular oxygen (air) has been used for this purpose as an electron acceptor for prevention of electron hole recombination. One approach used to prevent electron hole recombination is to add electron acceptors into the reaction media. The presence of H_2O_2 as electron acceptor can serve as electron scavengers to prevent the recombination and enhance photodegradation efficiency. H_2O_2 has several effects including: (a) avoid recombination of electron-hole by accepting the conduction band electron and (b) increase the concentrations of the hydroxyl radical[24].

$$H_2O_2 + h\upsilon \rightarrow 2^{\bullet}OH$$

$$h^+ + OH^- \rightarrow {}^{\bullet}OH^-$$

$$e^- + O_2 \rightarrow O_2^{-\bullet}$$

$$e^- + H_2O_2 \rightarrow HO^{\bullet} + OH^-$$

$$\text{Dye molecules} + {}^{\bullet}OH \rightarrow H_2O + \text{dye}^{\bullet} \rightarrow \text{further oxidation}$$

Furthermore, the enhanced degradation rate observed with H_2O_2 is probably due to direct photolysis by UV light. This generates $^{\bullet}OH$ radicals, which are likely to be dominant rate improving mechanism in the process. H_2O_2 has two hydrogen atoms bounded to oxygen atoms (H-O-O-H), thus it is more electropositive than O_2, suggesting that H_2O_2 is a better electron acceptor than oxygen. However, when present at high concentration, H_2O_2 also becomes a scavenger of both the valence band holes and hydroxyl radicals as follows[25].

$$H_2O_2 + 2h^+_{VB} \rightarrow O_2 + 2H^+$$

$$H_2O_2 + OH^{\bullet} \rightarrow HO^{\bullet}_2 + H_2O$$

$$HO^{\bullet}_2 + OH^{\bullet} \rightarrow H_2O + O_2$$

Effect of $K_2S_2O_8$

The effect of $K_2S_2O_8$ on the photodegradation of dyes was studied by addition of $K_2S_2O_8$ and keeping the other factors as constant. Peroxydisulphate anion $(S_2O_8)^{2-}$ is considered as a strong oxidizing agent and can be activated by means of UV/Solar irradiation, heat energy, transition metal ions or ultrasound irradiation to produce sulphate radicals ($SO_4^{\bullet-}$) as a stronger oxidizing agent with a redox potential of 2.6 V[26].

As can be seen from the above tables and graphs, it indicates that the increasing the concentration of $K_2S_2O_8$, the decolorization efficiency increases with in 60 min. This result can be explained by the following mechanisms. Firstly, sunlight irradiation can activate the $S_2O_8^{2-}$ ions as illustrated.

$$S_2O_8^{2-} + h\gamma \rightarrow 2SO_4^{\bullet-}$$

In the next step, hydroxyl radicals may be formed through sulphate radicals can be seen below Eq[27].

$$SO_4^{\bullet-} + H_2O \rightarrow H^+ + SO_4^{2-} + OH^{\bullet}$$

Furthermore, produced sulphate radicals can contribute in the degradation of organic dyes as shown through below Eq[28, 29].

$$SO_4^{\bullet-} + \text{Dye molecules} \rightarrow SO_4^{2-} + \text{Intermediates} + H^+$$

$$SO_4^{\bullet-} + \text{Intermediates} \rightarrow SO_4^{2-} + CO_2 + H_2O + \text{Other degradated products}$$

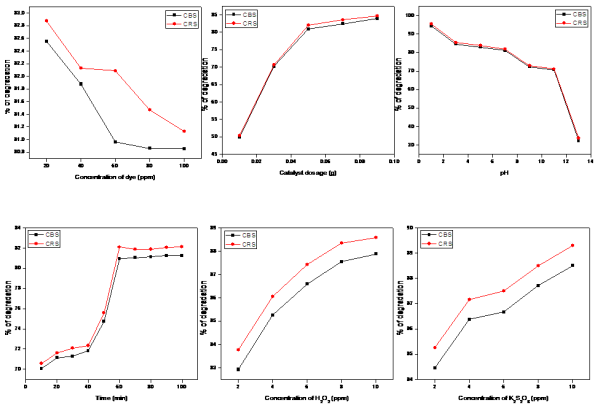

Fig.9. % of degradation vs Variable parameters

CONCLUSION

The results of this study demonstrate that comparison of photocatalytic activity of CRS and CBS has clearly indicated that the CRS is the most active photocatalyst for degradation of aniline blue dye solution. The initial rate of photodegradation increased with the increase of the catalyst dose up to an optimum loading. As the initial concentration of dyes was increased, the rate of degradation decreased in dye due to the decrease of the concentration OH^- adsorbed on catalyst surface. The

increasing of dye concentration increases the competitions between OH^- and dye to adsorb on active site of catalyst. Photocatalytic activity of anionic dyes (AB) reaches a maximum value in lower zero point charge. Sunlight has all type of radiation and so solar light can be efficiently used for the photo catalytic degradation of waste water. UV source is not only hazardous but also expensive because of large input of electric power to generate UV irradiation. In tropical countries like India, in large sunlight is available throughout the year and hence it could be efficiently used for Photocatalytic degradation of pollutants in waste water. Moreover CRS and CBS which are naturally available, low cost and effective are used as a photocatalyst.

REFERENCES

1. MahdaviTalarposhti A, Donnelly T and Anderson GK, Colour removal from a simulated dye wastewater using a two-phase anaerobic packed bed reactor. Water Research. 2001; 35(2): 425.
2. Hudlicky M. “Reduction in Organic Chemistry”. Halsted press: New York; 1984.
3. Arslan I and AkmehmetBalcioglu I, Degradation of commercial reactive dyestuffs by heterogenous and homogenous advanced oxidation processes: a comparative study. Dyes and Pigments. 1999; 43: 95-108.
4. Galindo C, Jacques P and Kalt A, Photooxidation of the phenylazonaphthol AO20 on TIO2: kinetic and mechanistic investigations. Chemosphere. 2001; 45: 997-1005.
5. Slokar YM and Le MarechalAM, Methods of Decoloration of Textile Wastewaters. Dyes Pigments. 1998; 37: 335-356.
6. Konstantinou IK and Albanis TA, TiO2-assisted photocatalytic degradation of azo dyes in aqueous solution: kinetic and mechanistic investigations: a review. Appl. Catal. B. 2004; 49: 1-14.
7. Oussi D, Mokrini A and Esplugas S, Removal of aromatic compounds using UV/H2O2. J. Photochem. Photobiol. A: Chem. 1997; 1: 77–83.
8. KumudMalikaTripathi, Tuan Sang Tran, Yoon Jin Kim, and TaeYoung Kim, Green Fluorescent Onion-Like Carbon Nanoparticles from Flaxseed Oil for Visible Light Induced Photocatalytic Applications and Label-Free Detection of Al(III) Ions. ACSSustain Chem Eng. 2017; 5(5): 3982-3992.
9. AnkitTyagi, KumudMalikaTripathi, Narendra Singh, ShashankChoudhary, and Raju Kumar Gupta, Green synthesis of carbon quantum dots from lemon peel waste: Applications in sensing and photocatalysis. RSC Adv. 2016; 6(76): 72423-72432, (2016).

10. Amy L. Linsebigler, Guangquan Lu, and John T. Yates Jr,Photocatalysis on TiO_2 Surfaces: Principles, Mechanisms, and Selected Results. Chem Rev.1995; 95(3): 735-758.
11. Ahmed S, Rasul MG, Brown R and Hashib MA, Influence of parameters on the heterogeneous photocatalytic degradation of pesticides and phenolic contaminants in wastewater: a short review. J Environ Manage. 2011; 92(3):311-330.
12. Michael R. Hoffmann, Scot T. Martin, Wonyong Choi, and Detlef W. Bahnemannt, Environmental Applications of Semiconductor Photocatalysis. Chem. Rev. 1995; 95:69-96.
13. Chen H, Nanayakkara CE and Grassian VH, Titanium dioxide photocatalysis in atmospheric chemistry. Chem. Rev. 2012; 112:5919-5948.
14. Miguel Pelaez, Nicholas T. Nolan, Suresh C. Pillai, Michael K. Seery, PolycarposFalaras, Athanassios G. Kontos, Patrick S.M. Dunlop, Jeremy W.J. Hamilton, J.Anthony Byrne, Kevin O'Shea, Mohammad H. Entezari and Dionysios D. Dionysiou, A review on the visible light active titanium dioxide photocatalysts for environmental applications. Appl. Catal. B.2012; 125: 331- 349.
15. T.P. Sharma, D. Patidar, N.S. Saxena, K. Sharma, T.P. Sharma, D. Patidar, N.S. Saxena and K. Sharma, Measurement of structural and optical band gaps of $Cd_{1-x}Zn_xS$ (x = 4 and 6) nanomaterials. Indian Journal of Pure and Applied Physics. 2006; 44: 125-128.
16. Haberhauer G and Gerzabek MH, Drift and transmission FT-IR spectroscopy of forest soils: an approach to determine decomposition processes of forest litter. Vibrational Spectroscopy. 1999; 19(2): 413-417.
17. Pragnesh N. Dave and Lakhan V. Chopda, Application of Iron Oxide Nanomaterials for the Removal of Heavy Metals. Journal of Nanotechnology. 2014; 1: 1-14.
18. Fan Jun, JiXin, Zhang Weiguang and Yan Yunhui, CJI.2004; 6(7): 45-49.
19. Ashwani Sharma, Sanjay Kumar, NarenderBudhiraja, Rajesh and Mohan Singh, Effect of calcination on morphology and optical properties of AlO-ZnOnanocomposites. Advances in Applied Science Research.2013; 4(2): 252-258.
20. Arup roy and Jayantabhattacharya, Microwave-assisted synthesis and characterization of cao nanoparticles. International Journal of Nanoscience. 2011; 10(3): 413-418.
21. Mahalakshmi M, Priya SV, Arabindoo B, Palanichamy M and Murugesam V, Photocatalytic degradation of aqueous propoxur solution using TiO2 and Hβ zeolite-supported TiO2. Journal of Hazardous materials. 2009; 161: 336–343.
22. Prakash D. Vaidya and Vijaykumar V. Mahajani, Insight into heterogeneous catalytic wet oxidation of phenol over a Ru/TiO2 catalyst. Chemical Engineering Journal.2002; 87: 403–416.

23. HindaLachheb, Eric Puzenat, AmmarHouas, Mohamed Ksibi, ElimameElaloui, Chantal Guillard and Jean-Marie Herrmann, Photocatalytic degradation of various types of dyes (Alizarin S, Crocein Orange G, Methyl Red, Congo Red, Methylene Blue) in water by UVirradiatedtitania. Applied Catalysis B: Environmental. 2002; 39: 75-90.
24. IsilGultekin and Nilsun H. Ince, Degradation of Reactive Azo Dyes by UV/H2O2: Impact of Radical Scavengers. Journal of Environmental Science and Health Part A. 2004; 39(4): 1069-1081.
25. So CM, Cheng MY, Yu JC and Wong PK, Degradation of azo dye Procion Red MX-5B by photocatalytic oxidation. Chemosphere. 2002; 46(6): 905-912.
26. Hou L, Zhang H and Xue X, Ultrasound enhanced heterogeneous activation of peroxydisulfate by magnetite catalyst for the degradation of tetracycline in water. Separation and purification Technology. 2012;84: 147-152.
27. Chen Y, Hu C, Qu JH and Yang M, Photodegradation of tetracycline and formation of reactive oxygen species in aqueous tetracycline solution under simulated sunlight irradiation. Journal of Photochemistry and Photobiology A: Chemistry. 2008; 197(1): 81-87.
28. Wen-Shing Chen and Yi-Chang Su, Removal of dinitrotoluenes in wastewater by sono-activated persulfate. UltrasonicsSonochemistry. 2012; 19: 921-927.
29. AlirezaKhataee, Reza DarvishiCheshmehSoltani, YounesHanifehpour, MahdieSafarpour, HabibGholipourRanjbar and Sang Woo Joo, Synthesis and Characterization of Dysprosium-Doped ZnO Nanoparticles for Photocatalysis of a Textile Dye under Visible Light Irradiation. Ind. Eng. Chem. Res. 2014; 53(5): 1924-1932.